5-2022

Acoustofluidic delivery of gene editing compounds for improved immunotherapy processing.

Riyakumari K. Patel
University of Louisville

ACOUSTOFLUIDIC DELIVERY OF GENE EDITING COMPOUNDS FOR IMPROVED IMMUNOTHERAPY PROCESSING

By

Riyakumari K. Patel
B.S. Bioengineering, University of Louisville, May 2021

A Thesis
Submitted to the Faculty of the
University of Louisville
J.B. Speed School of Engineering
as Partial Fulfillment of the Requirements
for the Professional Degree

MASTER OF ENGINEERING

Department of Bioengineering

April 2022

ACKNOWLEDGEMENTS

I would first like to thank my thesis committee members for their guidance, time, and knowledge for this project. This thesis would not have been possible without your endless support.

Dr. Jonathan Kopechek Dr. Patricia Soucy Dr. Kavitha Yaddanapudi

I would like to thank Dr. Jonathan Kopechek, who has served as a knowledgeable, patient, passionate, and kind mentor throughout my undergraduate and graduate studies. Dr. Kopechek gave me an opportunity for co-op in his lab, and he has since been a steady source of guidance. I am grateful for the knowledge and opportunities you have provided me. I have grown as a student, researcher, and curious mind in your lab.

Additionally, I would like to thank the many members of Dr. Jonathan Kopechek's lab who have guided me throughout the years. Mariah and Connor, thank you for teaching me technical lab skills and showing me how to design and conduct experiments. I appreciate the following lab members' help, guidance, and friendship.

Mariah Priddy Connor Center John Moore

I would like to thank all the BE faculty at the University of Louisville for providing me with the technical knowledge required to complete my thesis. I would also like to thank the friends I have made throughout the years, without whom I would not be here.

Lastly, thank you to my friends and family for their support and motivation throughout my studies. My friends and family have always pushed me to do my best and have believed in me throughout my highs and lows.

ABSTRACT

Cell-based immunotherapies are a new generation of "living-drug" treatments for cancer and other diseases. Chimeric antigen receptor (CAR) T-cell cancer therapy has shown promising results in lymphoma and B-cell malignancies. Currently, there are six FDA-approved CAR-T drugs on the market, and all of them use viral transfection for reprogramming. While viral transfection is effective, there are safety concerns due to inconsistent transfection that limit the use of CAR-T therapy. Current non-viral transfection techniques generally have lower transfection efficiency than viral transfection. Additionally, these techniques can be toxic, time-consuming, non-transportable, and expensive. To address these limitations, a novel 3D printed acoustofluidic system is being explored for inducing intracellular molecular delivery of therapeutic compounds for genetic editing. This system utilizes sonoporation, which creates reversible pores in the cell membrane when ultrasound waves rupture microbubbles. A solution of cells, microbubbles, and molecules of interest pass through fluidic channels and microbubbles rupture once exposed to ultrasound waves. A shockwave is created, which propels nearby material into the cell within seconds. In this thesis, several studies were conducted to assess the acoustofluidic mediated intracellular molecular delivery of compounds such as 150kDa FITC-Dextran, fluorescently labeled tracrRNA, and green fluorescent protein (GFP) in multiple cell lines. These studies indicate that cationic microbubbles alongside acoustofluidic treatment significantly increase intracellular molecular delivery of several different compounds. These studies show promise for the use of 3D printed acoustofluidic device for non-viral transfection of CRISPR/Cas9 in CAR-T cell processing.

TABLE OF CONTENTS

LIST OF FIGURES

I. INTRODUCTION

Objective

This thesis aims to assess the efficiency of a 3D-printed acoustofluidic device for the molecular delivery of various fluorescent compounds into four cell types. The long-term goal is to develop new acoustofluidic techniques to improve cell processing methods for immunotherapies.

Overview of CAR-T and Molecular Delivery

Cell-based immunotherapies are a growing field for the treatment of cancers and other diseases. Chimeric Antigen Receptor-T cell (CAR-T) therapy utilizes gene transfections techniques to re-program T-cells with desired surface markers and antigens (Figure 1). CAR-T cells are activated once they recognize the target antigen or surface marker on cancer cells and release chemokines and inflammatory cytokines to eliminate the cancer cell. A blood sample is received from the patient, and T-cells are isolated from the blood sample to re-engineer those T-cells with a specific CAR gene to express the desired function. Then the re-engineered cells are proliferated ex vivo before patient re-infusion.

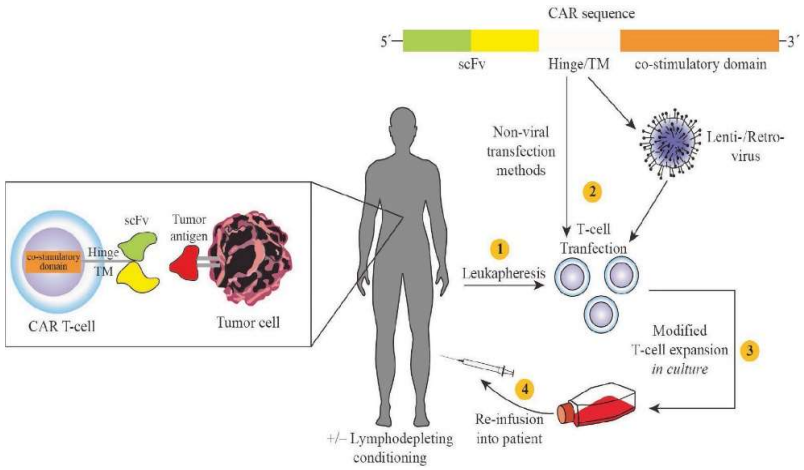

Figure 1: CAR-T cell processing steps are shown in this graphical representation from leukapheresis, T-cell transfection, T-cell expansion ex-vivo, and reinfusion of CAR-T cells in the patient [1].

Current cancer treatments include surgery, chemotherapy, and radiation. CAR-T therapy is an alternative treatment option for patients who may not respond well to current treatment plans. CAR-T is an exciting option for patients because it is a “living drug” targeted for patient-specific cancer. The essential components of CAR-T include an extracellular antigen recognition domain, a transmembrane domain, and an intracellular signaling domain [2]. CAR-T therapy was first approved for cancer treatment in 2017. Currently, there are six FDA-approved CAR-T products: Yescarta (Axi-cel), Kymriah (Tisa-cel), Breyanzi(Liso-cel), and Tecartus(Brexu-cel), Abecma (ide-cel) and Carvykti(Cilta-cel) are approved for leukemia, lymphoma, and multiple myeloma treatment [3-5]. These drugs use lentiviral or retroviral transfection to express anti-CD-19/CD-38/B-cell maturation antigens on the CAR. Target cancer-specific antigen, and upon activation, CAR-T cells are prompted to proliferate in-vivo and attack the cancer cells. CD-19 is an attractive surface marker for B-cell malignancies, such as leukemia or lymphoma, because it is expressed in all stages of B-cell differentiation [6, 7]. CAR-T therapy has shown promising results and provides a new therapeutic option, especially for patients with relapsed/refractory lymphoma; however, there are safety concerns and manufacturing challenges.

CAR-T cell therapy has several side effects with varying intensities. Two of the significant side effects are cytokine release syndrome (CRS) and neurotoxicity. CRS is systemic inflammation in response to interleukins released by CAR-T cells. Patients are monitored for signs of CRS such as fever, hypotension, and hypoxia, which can take several days to develop. CAR-T-related neurologic toxicities can vary from mild cognitive defects and tremors to seizures and death. CRS and neurologic toxicities can be managed

with steroids, but early detection and careful monitoring are essential to avoid life-threatening complications [2]. Additionally, CAR-T therapy makes patients susceptible to infections due to a severely suppressed immune system.

Several types of gene transfection methods are utilized for T-cell processing: gamma retroviral and lentiviral transfection, electroporation, sonoporation, cationic lipid-based delivery, and squeeze technology. Viral transfection uses the nature of viruses in which they hijack the host replication process allowing them to supplement the host genetic code. Retroviral transfections utilize lentiviral or γretroviral vectors to deliver CAR transgene into T-cells. Retroviral and lentiviral transfections methods are currently the primary method for T-cell manipulation. Due to the nature of viral vectors, genes are inserted randomly, which can lead to undesired mutagenesis and oncogenesis. Although viral vectors are effective, there are mutagenesis safety concerns due to the variability in viral gene transfection, which leads to surface expression that is uneven [8].

Non-viral transfection methods include physical and chemical techniques such as electroporation, sonoporation, squeeze technology, and cationic lipid-based delivery. Non-viral transfection methods use a variety of nucleic acids for genetic manipulation, such as small DNA, large DNA molecules (plasmid DNA), and RNA (Ribozymes, Si RNA, m RNA) [9]. Electroporation is a transfection method that uses high voltage to create temporary holes in the cell membrane allowing the substance of interest to enter the cell. The delivery of the material is not dependent on the charge, and both small and large molecules have been successfully delivered with this technique. Additionally, transfection efficiency is lower for electroporation in comparison to viral transfection. The high voltage required for this technique can damage the cells, and the effects of high electricity on the

genetic profile have not been fully characterized yet [10]. This technique also requires special buffers that conduct current efficiently [11]. Sonoporation is a process that uses ultrasound waves to induce microbubble cavitation which permeabilizes the cell membrane (Figure 2). When microbubbles are exposed to ultrasound, they oscillate in response to the pressure difference. This rapid expansion and compression of the microbubbles will eventually result in microbubble rupture known as inertial cavitation. Shock waves from inertial cavitation cause temporary pores in the cell membrane that allows for intracellular delivery of nearby contents [12]. The pores formed from inertial cavitation are momentary and repair within seconds once ultrasound is turned off. This technique is a promising non-viral delivery method; however, widespread use of this technique is limited due to the ultrasound setup needed. A microfluidic-based technology known as cell squeeze utilizes high shear stress, exposing the cells to mechanical deformation as they pass through very narrow channels. This high shear stress creates temporary holes in the cell membrane that allows for nearby material to go inside the cells. A few moments later, the cell membrane is restored. This mechanical deformation technique has shown promising results in delivering a variety of cargo materials, such as RNA, DNA, and CRISPR [13]. A challenge of this technology is the clogging of the narrow channels due to cell aggregates or other materials. Clogged channels are a common problem with microfluidic devices, especially when scaled up for processing [14]. Cationic lipid-based delivery is a chemical mode of transfection, and it is referred to as lipofection

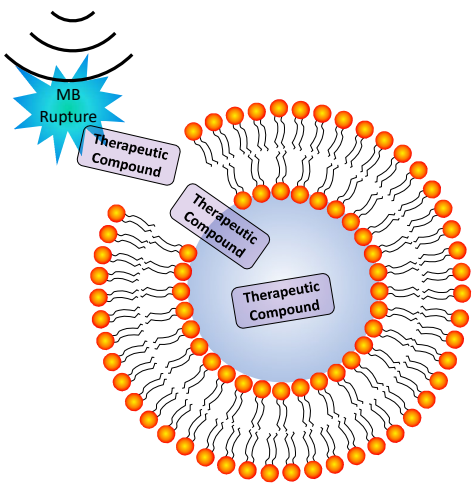

Figure 2: Illustration of Sonoporation Mechanism.

or lipid-mediated/liposome transfection. In this technique, positively charged liposomes interact with negatively charged DNA fragments and negatively charged cell membranes. The material of interest is delivered to the cells via endocytosis, and excess unnecessary materials are removed via exocytosis. This method has been proven effective for a wide range of cells and various cargo materials such as DNA, RNA, and proteins of different masses [10]. This technique has shown lower transfection efficiency in comparison to viral methods.

Despite the potential efficacy of viral and non-viral transfection techniques, non-specific random insertion of genes for CAR expression poses risks of accidental genetic mutations or highly variable CAR expression between cells which can adversely affect CAR-T treatment. Clustered regulatory interspaced short palindromic repeats (CRISPR) and corresponding protein Cas9 provide gene-specific transfection for CAR-T processing. CRISPR-Cas9 system uses a guide RNA to target the genome specifically, and Cas9 cuts off the guide RNA once it matches with the DNA of the host. Unlike current viral and non-viral transfection techniques that use nucleic acids for gene editing that are inserted randomly into the host genome, CRISPR/Cas9 allows for specific gene knockout/in [15]. CRISPR/Cas9 is expected to lower the side effects related to the current treatment with CAR-T, such as Cytokine release syndrome (CRS) and neurotoxicity. The use of CRISPR/Cas9 alongside viral transfection or other transfection methods such as the one proposed here will lead to a safer and more potent CAR-T product [16]. The use of CRISPR/Cas9 with CAR-T opens the possibility of allogeneic CAR-T cells, which can provide an off-the-shelf product [15]. Current CAR-T products are autologous and require the patient's T-Cells which can be challenging to acquire in cancer patients, lengthens the

manufacturing process, and a personalized product is more expensive than an off-the-shelf product. Precision genome editing with CRISPR/Cas9 will help overcome current obstacles because multiple genes can be targeted at once. The above-mentioned viral and non-viral techniques have been used to transduce CRISPR/Cas9 using viral transfection and electroporation [17]. While CRISPR/Cas9 systems address the problems such as CRS and neurotoxicity, challenges with current viral and non-viral transfection techniques still limit the use of CRISPR/Cas9 for CAR-T processing. Challenges with non-viral and viral transfection prevent the large-scale production of CAR-T cells.

Problem

Current techniques used for transfection of genetic materials in the processing of CAR-T cells present challenges that limit the use of this therapy. As mentioned above, both viral and non-viral techniques have presented their limitations and challenges. Thus, there is a need for a processing technique that delivers molecular compounds to T-cells effectively and consistently and has the potential to be scaled up for higher throughput. The 3-D printed acoustofluidic system discussed here holds the potential to address these limitations.

Bioengineering Solution: 3D Printed Acoustofluidic Device for Molecular Delivery

To address the limitations of current viral and non-viral gene-editing techniques, Dr. Jonathan Kopechek's laboratory at the University of Louisville is developing a 3D-printed acoustofluidic device for molecular delivery. This system utilizes an ultrasonic transducer with an acoustofluidic device to induce microbubble cavitation to permeabilize the cell membrane for intracellular delivery of therapeutic compounds (Figure 3).

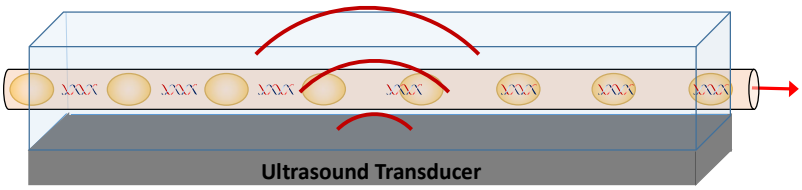

Figure 3: Schematic representation of how 3D printed acoustofluidic device mediated cell membrane rupture will allow intra-cellular uptake of surrounding molecular components.

Dr. Kopechek's lab first tested the use of sonoporation for molecular delivery with a clinical ultrasound probe. In this setup, the cell solution (cells, microbubbles, and biomolecules) was in a conical vial which was placed in a water tank. The water served as a medium for the ultrasonic waves to propagate. This technique was inefficient because the cells received inconsistent ultrasound exposure due to the shielding of some cells by microbubbles, and the ultrasound waves would attenuate before reaching the cells that were on the backside of the conical vial [18]. The following iteration of this system was an acoustofluidic device to provide consistent exposure to ultrasound. In this setup, the cell solution (cells, microbubbles, and biomolecules) is pushed through the 3D printed device with a peristaltic pump. A clinical ultrasound probe is placed directly above the acoustofluidic device with a layer of ultrasound gel which provides a medium for ultrasonic waves (Figure 4). The cells pass through a 1mm concentric spiral channel directly under the ultrasound probe. A concentric spiral design was chosen to optimize the cell exposure to ultrasound. Experimental studies using this 3D-printed acoustofluidic device for intracellular molecular delivery are discussed below.

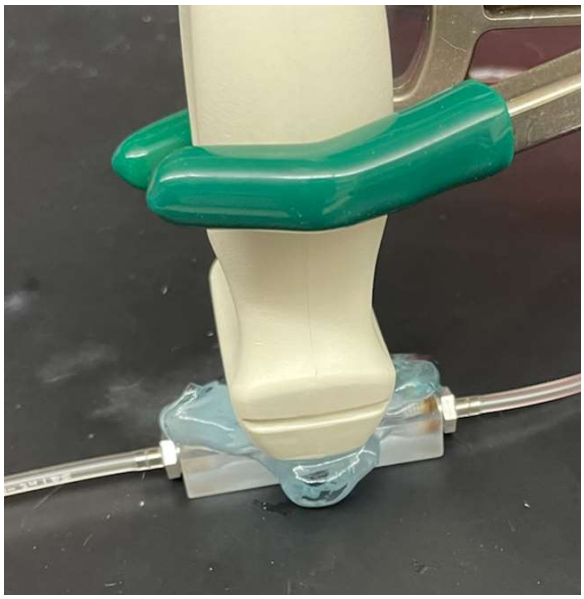

Figure 4: Set-up of 3D printed acoustofluidic device with ultrasound imaging probe.

II. METHODS

Cell culture and Harvesting

Jurkat T lymphocytes were cultured in complete RPMI-1640 medium (10% fetal bovine serum (FBS) and 1% penicillin/streptomycin) (Cytiva Life Sciences, Marlborough, MA, USA) at 37 °C and 5% CO_2 in a flat-bottom tissue culture flask. A549 cells, MDA-MB-231 cells, and HEK293 cells were cultured in complete DMEM medium with 10% fetal bovine serum (FBS) and 1% penicillin/streptomycin) (Cytiva Life Sciences) at 37 °C and 5% CO_2 in a flat-bottom tissue culture flask. To harvest, A549 cells, MDA-MB-231 cells, and HEK293 cells were washed once with PBS, and trypsin was added to release attached cells. After five minutes of incubation time, the cell/trypsin solution was neutralized with complete DMEM medium and collected into a conical vial. These cells were centrifuged at 1500g for 5 minutes at 4 °C. To harvest Jurkat T-lymphocytes, they were collected in conical vials and centrifuged at 1500g for 5 minutes at 4 °C. Cells were resuspended at a concentration of 100,000 cells/mL.

Microbubble Synthesis

Perfluorobutane gas-filled microbubbles were synthesized as previously described [19]. These gas-filled microbubbles were created with a cationic lipid solution and had a mean diameter of 2 ± 1 μm. Positively charged phospholipid-coated gas-filled microbubbles were used for these studies as they were previously shown to be necessary for effective acoustofluidic mediated molecular delivery[19-22]. Cationic microbubble lipid solution comprised of 1,2-distearoyl-sn-glycero-3-phosphocholine (DSPC, Avanti Lipids, Alabaster, AL, USA); 1,2-distearoyl-sn-glycero-3-ethylphosphocholine (DSEPC, Avanti Lipids); 1,2-distearoyl-sn-glycero-3-phosphoglycerol (DSPG, Avanti Lipids); and

polyethylene glycol-40 stearate (Sigma-Aldrich, St. Louis, MO, USA) at molar ratios of 100:43:1:4.5. Microbubbles with neutral surface charge were formulated with chloroform solutions of DSPC and 1,2 distearoyl-sn-glycerol-3-phosphoethanolamine-N-[amino(polyethylene glycol0 -2000] (DSPC-PEG-2000, Avanti Lipids) at a molar ratio of 96:4[23]. These lipids were combined in a 20-mL glass vial and desiccated until all the chloroform was removed. The dry lipid film was resuspended in 1x PBS and sonicated (Qsonica, Newtown, CT, USA) to create an aqueous micellar lipid solution at a concentration of 10mg/mL. The lipid solution was diluted in 4x PBS in a 2-mL glass vial and sealed to produce microbubbles. The air in the headspace of the glass vial was replaced with decafluorobutane gas (FlouroMed, Round Rock, TX, USA). The glass vial was then amalgamated at 4350 cpm for 45 seconds (DB-338, COXO, Foshan City, China) to form cationic microbubbles.

Trans-activating CRISPR RNA(tracrRNA) is one of three components of the CRISPR/Cas9 system used for genome editing in cultured cells. To perform CRISPR/Cas9 genome editing, a CRISPR RNA(identifies the target DNA sequence) must bind to a tracrRNA, activating the Cas9 endonuclease to create a functional editing ribonucleoprotein complex. The tracrRNA used in our studies was fluorescently labeled with ATTO550 to allow for analysis via flow cytometry. To form microbubbles with Alt-R CRISPR/Cas9 tracrRNA, ATTO 550(IDT Technologies, USA) the steps mentioned above were followed. To produce tracrRNA-ATTO550 microbubbles the lipid solution and tracrRNA-ATTO550 solution was diluted in PBS to a concentration of 5μg/mL in a 2-mL glass vial and sealed. The air in the headspace of the glass vial was replaced with decafluorobutane gas (FlouroMed, Round Rock, TX, USA). The glass vial was then

amalgamated at 4350 cpm for 45 seconds (DB-338, COXO, Foshan City, China) to form cationic microbubbles. These steps were followed to create a tracrRNA-ATT50 diluted solution without any gas or amalgamation steps.

Acoustofluidic Device Manufacturing

3D printed acoustofluidic device was designed in SolidWorks (Waltham, MA, USA) and driven by a peristaltic pump. A 1mm x 1mm concentric spiral channel design was chosen based on prior experiments for optimal molecular delivery (Figure 5) [20]. The flow chamber was created using stereolithography 3D printing (Xometry, Gaithersburg, MD, USA) on Accura 60 plastic. Inlet and outlet openings of the flow chamber were threaded with stainless steel barbed tube fittings (10-32 threads, McMaster-Carr, Elmhurst, IL, USA) to link to PVC tubing (1/16" ID, McMaster-Carr). A peristaltic pump was used to push the cell solution through the device at a flow rate of 1.5mL/min (Boxer GmbH, Ottobeuren, Germany). An ATL P4-1 ultrasound transducer was placed directly above the concentric spiral channel on the 3D-printed acoustofluidic device. A thin layer of ultrasound gel was applied to the transducer and the acoustofluidic device to allow for acoustic coupling. Verasonics Vantage 64LE ultrasound imaging system was used to generate B-mode pulses at a frequency of 2.5MHz.

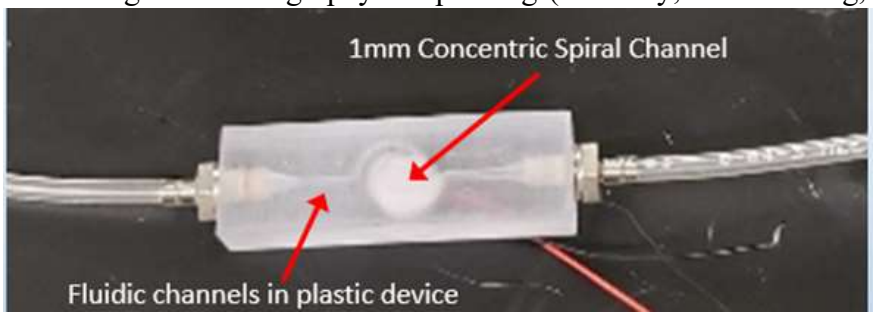

Figure 5: 3D printed acoustofluidic device with the concentric spiral channel design in the center of the device.

Molecular Delivery to Human Cells

A mixture of cationic microbubbles, the fluorescent molecule of interest (tracrRNA ATTO-550), and Jurkat cells or HEK293 cells was pumped through the 3D printed acoustofluidic system to expose the cells to ultrasound. Cationic microbubble and tracrRNA-ATTO550 solution were added to the cell solution at a concentration of 5% v/v before acoustofluidic treatment. After treatment, cells were collected and seeded in a 24-well plate at 37 °C and 5% CO_2 for 48 hours. After 48-hour incubation, cells were harvested as described above and washed via centrifugation three times with PBS to remove any remaining extracellular compounds.

FITC Dextran Delivery to Multiple Cell Lines

A mixture of cationic microbubbles, the fluorescent molecule of interest (150kDa FITC-Dextran), and either Jurkat cells, A549 cells, MDA-MB-231 cells, or HEK293 cells, was pumped through the 3D printed acoustofluidic system to expose the cells to ultrasound. 1.5mM 150kDa FITC-Dextran macromolecule was added to the cell and cationic microbubble solutions directly before acoustofluidic treatment. Six concentrations of cationic microbubbles were tested 0% v/v to 10.0% v/v. After acoustofluidic treatment, cells were washed via centrifugation three times with PBS to remove extracellular FITC-Dextran and other debris. Propidium iodide (PI) stain was added to the cells to determine cell viability before flow cytometry analysis.

GFP Delivery to Jurkat T-cells

A mixture of Jurkat cells, cationic microbubbles, and GFP (28kDa) was pumped through the 3D printed acoustofluidic system to expose the cells to ultrasound. GFP (2 μM)

was directly added to the cell and cationic microbubble solutions before acoustofluidic treatment. After acoustofluidic treatment, cells were washed via centrifugation three times with PBS to remove extracellular GFP and other debris. Propidium iodide (PI) stain was added to the cells before flow cytometry analysis to exclude non-viable cells.

Flow Cytometry Analysis

Intracellular molecular delivery was determined through the detection of fluorescent compounds with a flow cytometer (MACSquant, Miltenyi Biotec, Bergisch Gladbach, Germany). Flow cytometry channels were chosen based on appropriate wavelengths for the fluorescent molecule of interest. Flow cytometry software, FlowJo (FlowJo, Ashland, OR USA) was used to analyze flow cytometry data. Forward and side scattering was used to gate live cells based on size and granularity. A histogram was created to display the fluorescence intensity of the molecule of interest, the x-axis was the logarithmic fluorescence intensity value, and the y-axis was the cell count. Mean fluorescence intensity was calculated from the histogram. The average, standard deviation, and fold change of these values were calculated in Microsoft Excel.

Statistical Analysis

Statistical analysis was performed using Minitab (State College, PA) and MS Excel. A one-way variance (ANOVA) test was utilized to compare multiple groups. Post-hoc analysis was used for comparison between groups with a Tukey's test. A p-value less than 0.05 was defined as statistically significant. Bars on the figures are representative of means ± standard errors.

III. RESULTS AND DISCUSSION

Effect of Microbubble Concentration on Acoustofluidic Molecular Delivery in Different Cell Lines

Acoustofluidic mediated molecular delivery of a fluorescent macromolecule 150kDa FITC-Dextran (1mM) was tested in four cell lines at six different cationic microbubble concentrations. The following cell lines were tested: Jurkat T-cells Human lymphocytes, MDA-MB-231 human breast carcinoma cells, human A549 lung carcinoma cells, and HEK293 cells were tested at microbubble concentrations of 0%-10% v/v. The cells were treated with acoustofluidic treatment and appropriate microbubble concentration. Post-treatment, the cells were washed three times, and propidium iodide (PI) stain was added before flow cytometry analysis. PI stain was used as an indicator of non-viable cells, and this measurement was used to calculate cell viability. Results of these experimental trials are shown below in figures 5-8.

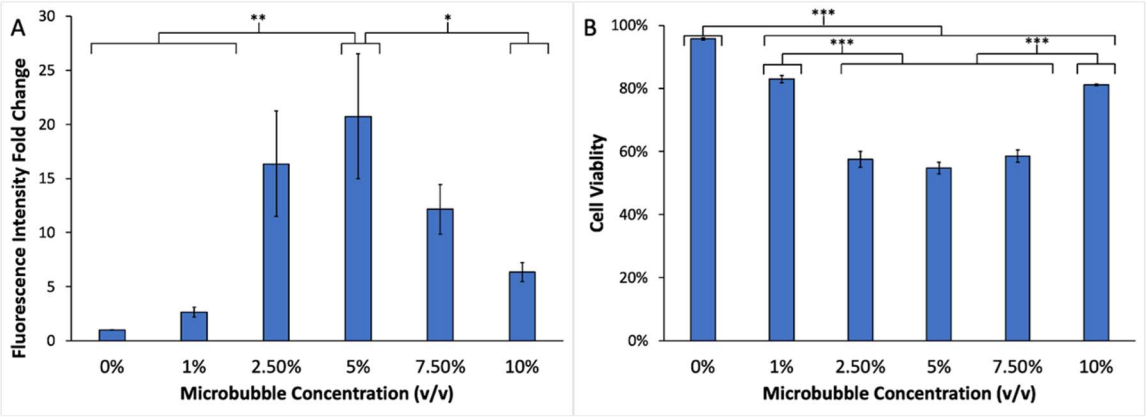

Figure 6: (A) Cationic microbubble concentration of 5% v/v significantly enhanced molecular delivery of 150kDa FITC-Dextran(1mM) to Jurkat T-cells. (B) Cell viability of Jurkat T-cells was significantly reduced after acoustofluidic treatment for all microbubbles concentrations compared to the control group with no microbubbles.

Figure 6 shows the effects of different microbubble concentrations on acoustofluidic mediated molecular delivery of 150kDa FITC-Dextran in Jurkat T-cells. Intracellular delivery was significantly enhanced at a microbubble concentration of 5% v/v when compared to concentrations of 0-1% v/v (ANOVA $p<0.01$, n=6/group) and 10% v/v ($p<0.05$). Effects of microbubble concentration on cell viability, as indicated by the absence of PI stain, are shown in Figure 5B. Acoustofluidic treatment significantly reduced cell viability for all microbubble concentrations compared to the negative control group with no microbubbles (ANOVA $p<0.001$, n=6/group). Furthermore, acoustofluidic treatment at microbubble concentrations of 2.5% v/v – 7.5% v/v significantly reduced cell viability in comparison to microbubble concentrations of 1% v/v and 10% v/v ($p<0.001$).

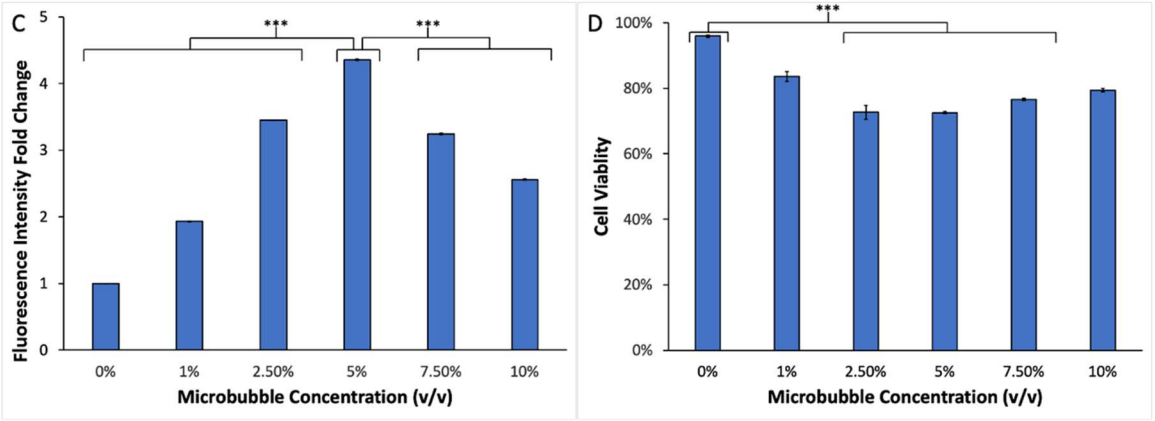

Figure 7: (C) Cationic microbubble concentration of 5% v/v significantly enhanced molecular delivery of 150kDa FITC-Dextran(1mM) to MDA-MB-231 cells. (D) Cell viability of MDA-MB-231 cells was significantly reduced after acoustofluidic treatment for microbubble concentrations of 2.5%-7.5% v/v compared to the control group with no microbubbles.

Figure 7 shows the effects of different microbubble concentrations on acoustofluidic mediated molecular delivery of 150kDa FITC-Dextran (1mM) in MDA-MB-231 cells and the corresponding effects on cell viability. Intracellular molecular delivery of 150kDa FITC-Dextran was significantly enhanced at a microbubble concentration of 5% v/v in comparison to microbubble concentrations of 0%-2.5% v/v and

7.5% v/v (ANOVA p<0.001, n=6/group). Effects of microbubble concentration on cell viability, as indicated by the absence of PI stain, are shown in Figure 6D. Acoustofluidic treatment at microbubble concentrations of 2.5%-7.5% v/v reduced cell viability significantly compared to the negative control group with no microbubbles (p<0.001).

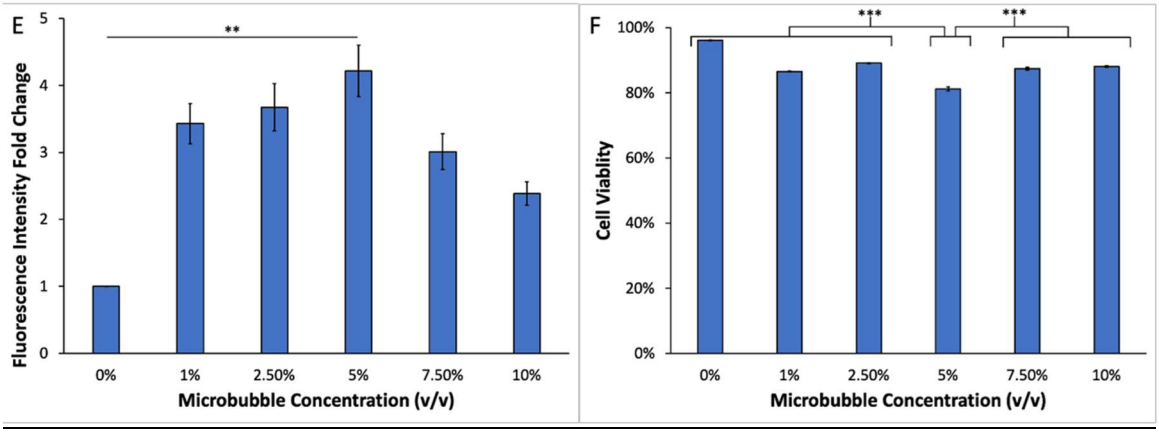

Figure 8: (E) Cationic microbubble concentration of 5% v/v significantly enhanced molecular delivery of 150kDa FITC-Dextran(1mM) to A549 cells. (F) Cell viability of A549 cells was significantly reduced after acoustofluidic treatment at a microbubble concentration of 5% v/v compared to microbubble concentrations of 0%-2.5% v/v and 7.5%-10% v/v.

Figure 8 shows the effects of different microbubble concentrations on acoustofluidic mediated molecular delivery of 150kDa FITC-Dextran (1mM) in A549 human lung carcinoma cells and the corresponding effects on cell viability. Intracellular molecular delivery of 150kDa FITC-Dextran was significantly enhanced at a microbubble concentration of 5% v/v compared to the negative control group with no microbubbles (ANOVA p<0.001, n=9/group). Effects of microbubble concentration on cell viability, as indicated by the absence of PI stain, are shown in Figure 7F. Acoustofluidic treatment at a microbubble concentration of 5% v/v reduced cell viability significantly compared to microbubble concentrations at 2.5%-7.5% v/v (p<0.001).

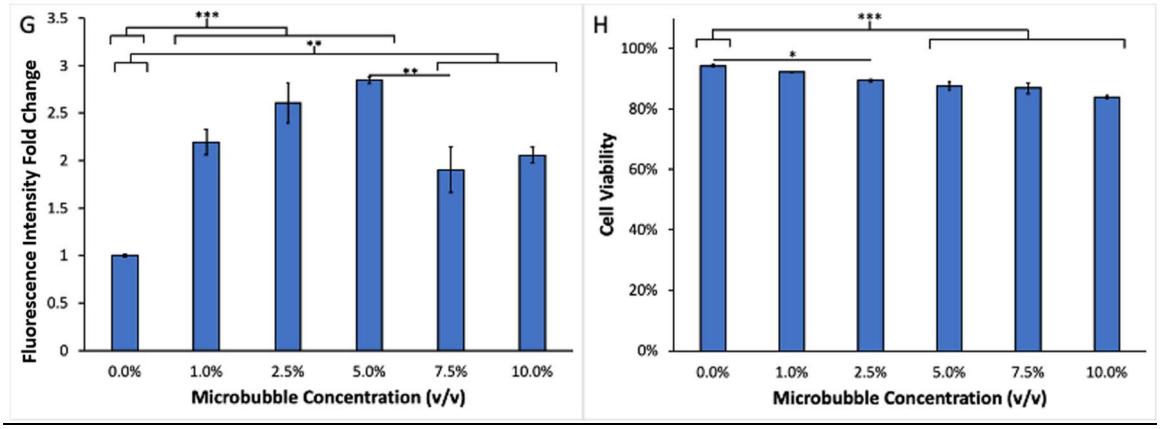

Figure 9: (G) Cationic microbubble concentration of 5% v/v significantly enhanced molecular delivery of 150kDa FITC-Dextran(1mM) to HEK293 cells. (H) Cell viability of HEk293 cells was significantly reduced after acoustofluidic treatment at microbubble concentrations of 2.5%-10%v/v compared to *the* control group with no microbubbles.

Figure 9 shows the effects of different microbubble concentrations on acoustofluidic mediated molecular delivery of 150kDa FITC-Dextran (1mM) in HEK293 cells and the corresponding effects on cell viability. Intracellular molecular delivery of 150kDa FITC-Dextran was significantly enhanced at all microbubble concentrations of 1-10% v/v compared to the negative control group with no microbubbles (ANOVA $p<0.01$, n=3-6/group). Effects of microbubble concentration on cell viability, as indicated by the absence of PI stain, are shown in Figure 8H. Acoustofluidic treatment at microbubble concentrations of 5%-10% v/v reduced cell viability significantly (ANOVA $p<0.01$, n=3-6/groups) and 2.5% v/v ($p<0.05$) when compared to the negative control group with no microbubbles. Additionally, cell viability remained above 80% for all groups.

TracrRNA Delivery to HEK293 Cells

Acoustofluidic mediated molecular delivery of a fluorescently labeled tracrRNA (ATTO-550) was tested in two different cell lines at varying conditions. A fluorescently labeled tracrRNA was used because successful intracellular delivery can be detected via

flow cytometry. tracrRNA is a ribonucleoprotein (RNP) that is an essential part of the CRISPR/Cas9 system. The cells were treated with acoustofluidic treatment at appropriate conditions, and all samples were washed after incubation and before flow cytometry was used to assess intracellular delivery. Results of these experiments in HEK293 cells and human lymphocytes Jurkat T-cells are shown below.

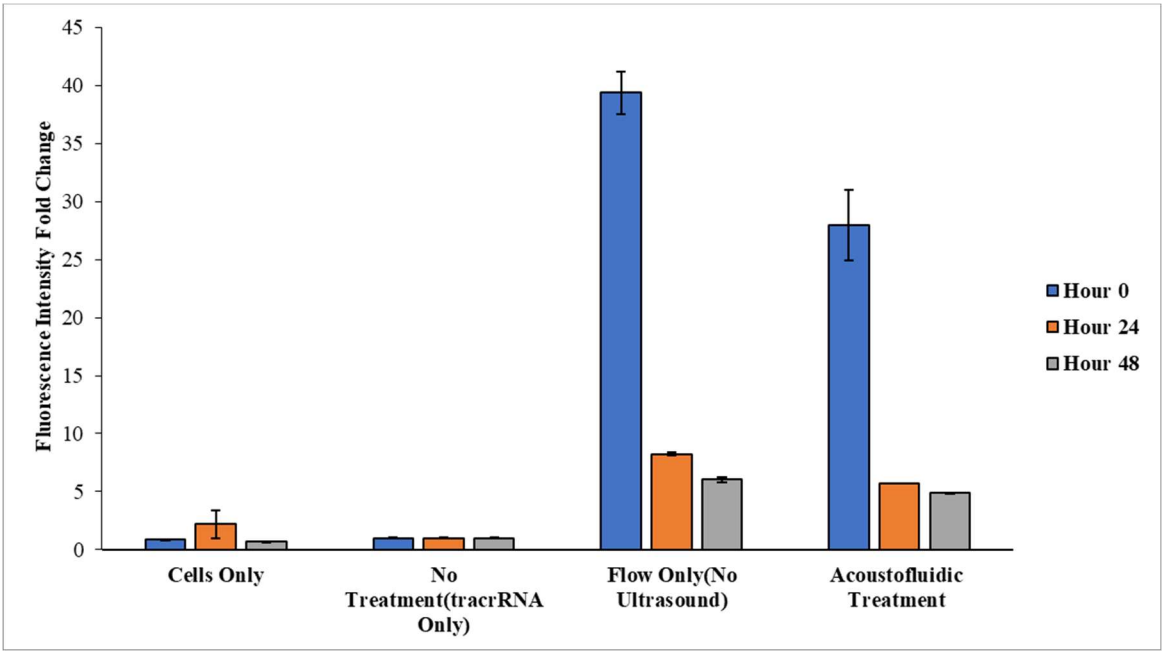

Figure 10: Cationic microbubbles (in both the flow only and the acoustofluidic treatment groups) significantly enhance tracrRNA uptake in HEK293 cells from 0 h- 48h with or without acoustofluidic treatment, compared to tracrRNA alone without microbubbles (n=3/group).

Figure 10 shows acoustofluidic mediated molecular delivery of tracrRNA in HEK293 cells over three different time points of zero hours, 24 hours, and 48 hours. All three-time points were statistically significant, as indicated by an ANOVA test and ANOVA p-value of ≤ 0.001 (n=3/group). Post-hoc analysis indicated that acoustofluidic treatment and flow only (no ultrasound) groups had significantly higher relative fluorescence when compared to cells only and no-treatment groups.

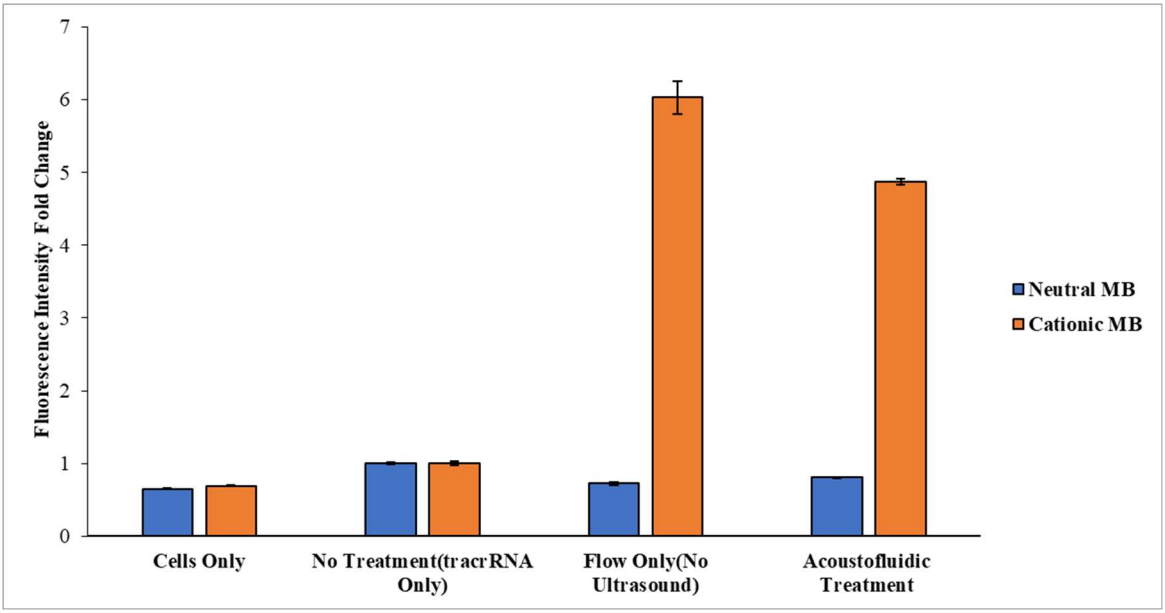

Figure 11: Cationic microbubbles (in both the flow only and the acoustofluidic treatment groups) significantly enhance tracrRNA uptake in HEK293 cells compared to neutral microbubbles, with or without acoustofluidic treatment (n=3/group).

Figure 11 shows acoustofluidic mediated molecular delivery of tracrRNA in HEK293 cells with cationic microbubbles and neutral microbubbles over an incubation period of 48 hours. These results are statistically significant, as indicated by an ANOVA p-value of ≤ 0.001 (n=3/group). Post-hoc analysis results found that cationic microbubbles with flow only (no ultrasound) and cationic microbubbles with acoustofluidic treatment had significantly higher relative fluorescence intensity when compared to the rest of the groups (including neutral microbubble flow only and acoustofluidic treatment groups). These results indicate that cationic microbubbles enhance intracellular uptake of tracrRNA in comparison to neutral microbubbles.

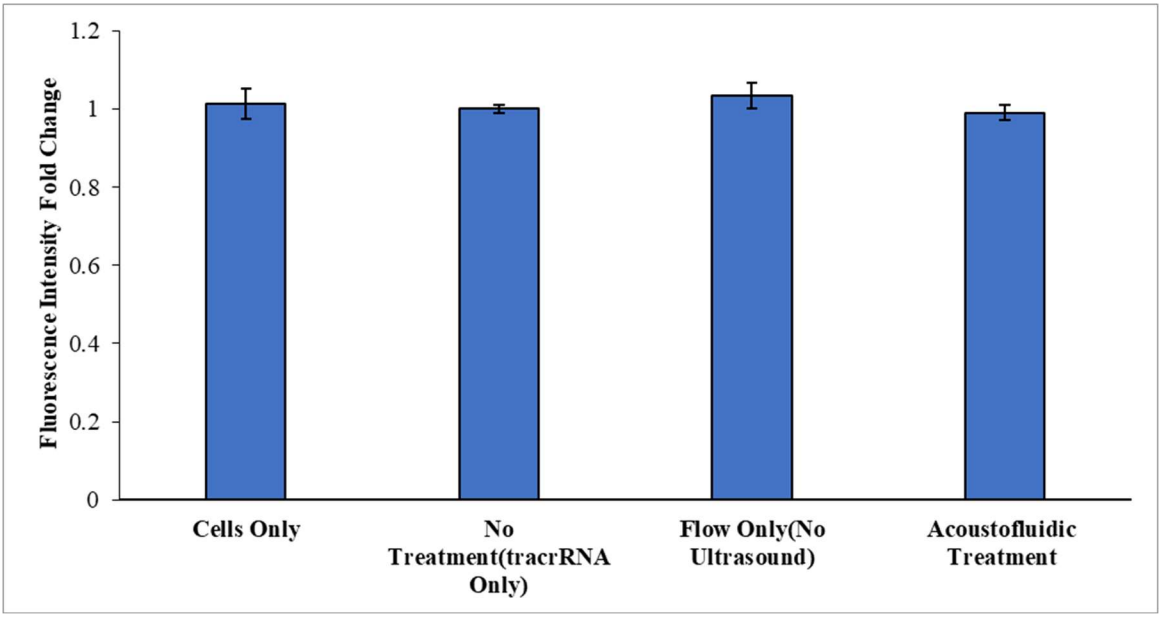

Figure 12: Washing HEK293 cells immediately after acoustofluidic treatment limits intracellular uptake of tracrRNA (n=6/group).

Figure 12 shows the effects of washing HEK293 cells directly after acoustofluidic treatment on molecular delivery of tracrRNA. The cells were treated with acoustofluidic treatment and washed three times with PBS following treatment to remove any extracellular compounds. ANOVA testing revealed these results not to be statistically significant as the p-value was not ≤ 0.05. These results indicate that washing cells immediately after acoustofluidic treatment prevents intracellular uptake of tracrRNA.

TracrRNA Delivery to Jurkat T-Cells

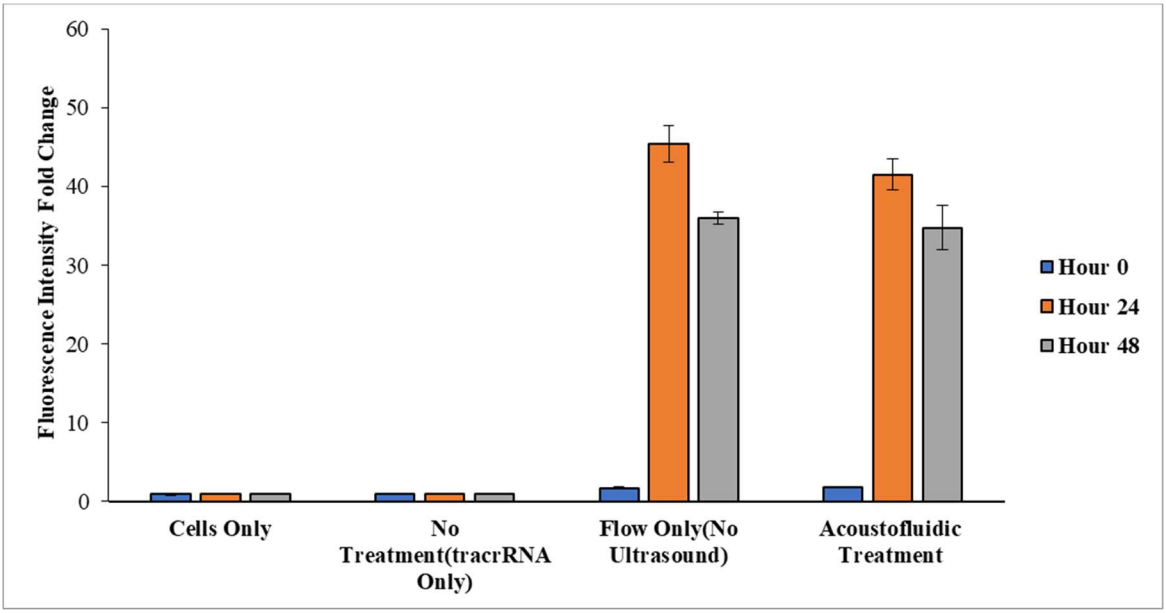

Figure 13: Cationic microbubbles significantly enhance tracrRNA uptake in Jurkat T-cells from 0 h- 48h with or without acoustofluidic treatment, compared to tracrRNA alone without microbubbles (n=2-3/group).

Figure 13 shows acoustofluidic mediated molecular delivery of tracrRNA in Jurkat T-cells over three different time points of zero hours, 24 hours, and 48 hours. All three times were statistically significant, as indicated by an ANOVA test and ANOVA p-value of ≤ 0.001(n=2-3/group). Post-hoc test results revealed that acoustofluidic treatment and flow only (no ultrasound) groups had significantly higher relative fluorescence intensity than cells only and no treatment (tracrRNA only) groups. These results indicate that flow only and acoustofluidic treatment both significantly enhance intracellular delivery of tracrRNA in Jurkat T-cells at all three-time points.

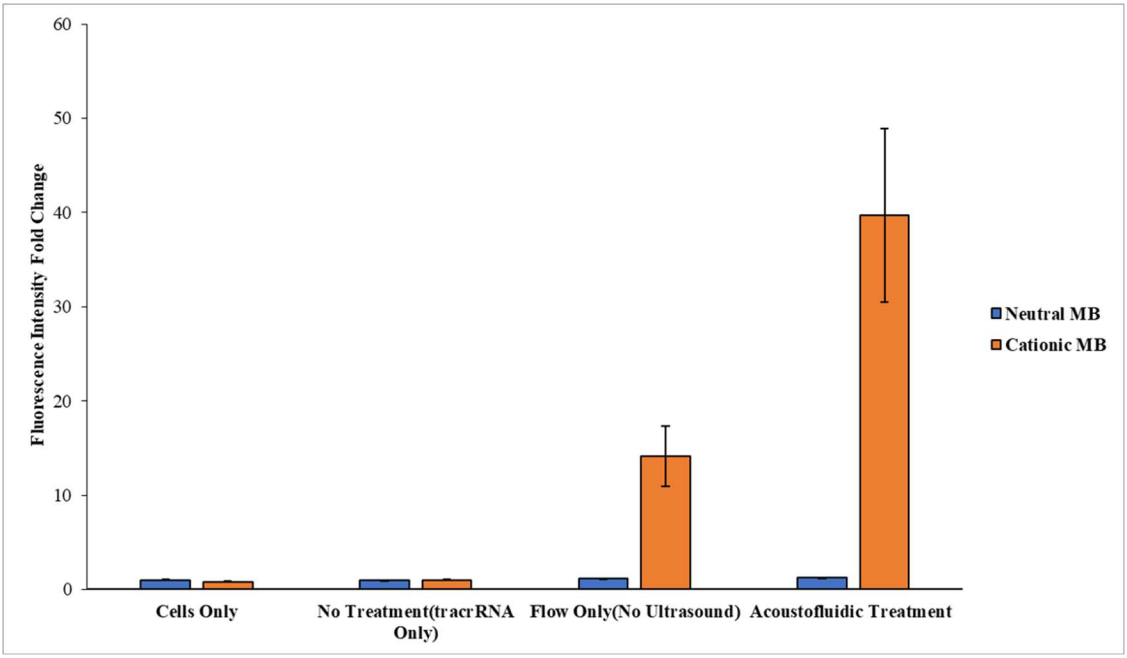

Figure 14: Cationic microbubbles significantly enhance tracrRNA uptake in Jurkat T-cells compared to neutral microbubbles, with or without acoustofluidic treatment (n=3-15/group).

Figure 14 shows acoustofluidic mediated molecular delivery of tracrRNA in Jurkat T-cells with cationic microbubbles and neutral microbubbles over an incubation period of 48 hours. These results are statistically significant, as indicated by an ANOVA p-value of ≤ 0.001(n=3-15/group). Post-hoc test results found that acoustofluidic treatment with cationic microbubbles had significantly higher relative fluorescence intensity when compared to the other groups. These results indicate that cationic microbubbles with acoustofluidic treatment enhance intracellular uptake of tracrRNA in comparison to neutral microbubbles and acoustofluidic treatment.

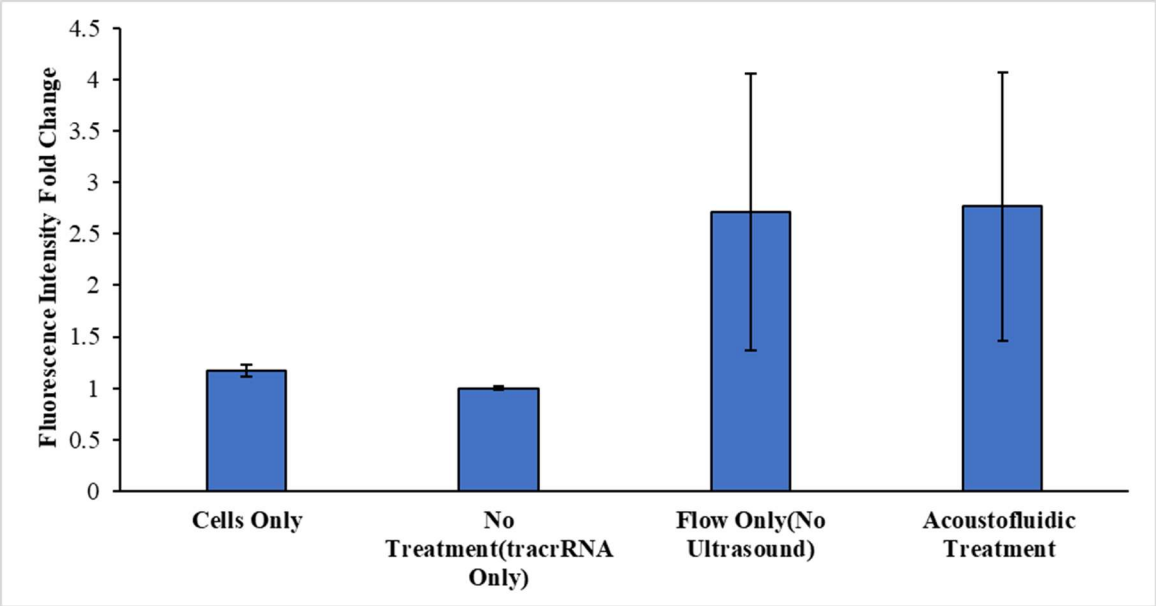

Figure 15: Washing Jurkat-T cells immediately after acoustofluidic treatment limits intracellular uptake of tracrRNA (n=5-6/group).

Figure 15 shows the effects of washing Jurkat T-cells directly after acoustofluidic treatment on molecular delivery of tracrRNA. The cells were treated with acoustofluidic treatment and washed three times with PBS following treatment to remove any extracellular compounds. ANOVA testing revealed these results not to be statistically significant as the p-value was not ≤ 0.05 (n=5-6/group). These results indicate that washing cells immediately after acoustofluidic treatment prevents intracellular uptake of tracrRNA.

Acoustofluidic mediated GFP Delivery to Jurkat T-Cells

Acoustofluidic mediated molecular delivery of green fluorescent protein (GFP) was tested in Jurkat T-cells. The cells were treated with acoustofluidic treatment as described in the methods section. Post-treatment, the cells were washed three times, and propidium iodide (PI) stain was added before flow cytometry analysis. PI stain was used as an indicator of non-viable cells, and this was used to calculate cell viability.

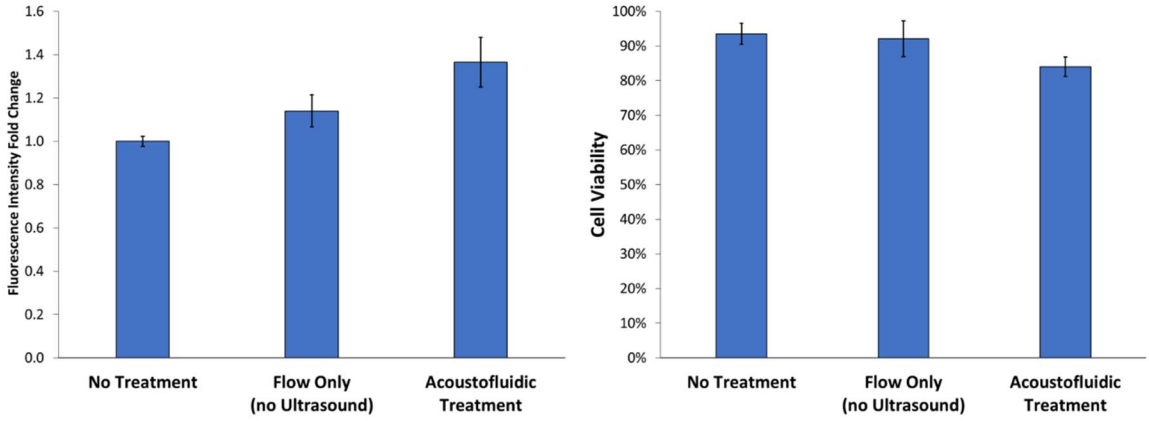

Figure 16: Acoustofluidic treatment significantly enhanced molecular delivery of GFP in Jurkat T-cells in comparison to no treatment group (n=3-6/group). Additionally, cell viability remained relatively high with acoustofluidic treatment.

Figure 16 shows the acoustofluidic mediated intracellular delivery of GFP in Jurkat T-cells. Acoustofluidic treatment significantly enhanced molecular delivery of GFP in comparison to the no treatment group ($p<0.001$, n=3-6/group). The flow-only group did not show a significant increase in fluorescence compared to the no-treatment group ($p=0.06$, n=3-6/group). Additionally, cell viability was not negatively impacted by acoustofluidic treatment as cell viability remained greater than 80% for all groups.

Discussion

The 3D-printed acoustofluidic system enhanced molecular delivery in various cell lines, as demonstrated by the studies conducted in this thesis. These results show promise that this 3D-printed acoustofluidic system may enable improved techniques for the non-viral processing of cells for gene therapy applications. The effects of varying microbubble concentrations on the efficiency of acoustofluidic mediated molecular delivery of macromolecule 150kDa FITC-Dextran and cell viability of four different cell lines were assessed to determine optimal microbubble concentrations. These four cell lines were used to test molecular delivery to determine differences between cell types. These cell lines had

different properties and characteristics that may affect molecular delivery, such as the cell size, shape, and whether these cells are in suspension or adherent during culture. Additionally, HEK293 cells are often recommended for transfection and are known to have a high transfection efficiency [24]. These preliminary studies were conducted with Jurkat T-cells to optimize molecular delivery before testing with primary T-cells. There was some variance in the results between cell lines, still, all cell lines showed significantly enhanced molecular delivery at microbubble concentrations of 5% v/v in comparison to the negative control group without microbubbles and ultrasound treatment. Furthermore, the cell viability decreased for all cell lines at a microbubble concentration of 5% v/v compared to the negative control group without microbubbles and without ultrasound treatment. However, cell viability remained relatively high for groups and cell types. Increased microbubble concentration, greater than 5% v/v, reduced intracellular delivery of 150kDa FITC-Dextran while maintaining relatively high cell viability. An increased microbubble concentration is generally linked to reduced cell viability due to cytotoxic effects [25]. A possible explanation of this trend is "shadowing" because of decreased microbubble oscillation due to increased scattering of ultrasound waves at higher concentrations of microbubbles (10% v/v). Previous studies have described similar trends with different cell lines and microfluidic devices [20, 26]. These results indicate an ideal "therapeutic window" of microbubble concentrations that enhance acoustofluidic mediated intracellular delivery of molecules. These results demonstrate that acoustofluidic treatment with cationic microbubbles is effective at intracellular molecular delivery of macromolecules such as 150kDa FITC-Dextran in multiple cell lines without dramatically compromising cell viability. 150kDa FITC-Dextran was chosen as the test molecule because it is a

fluorescent macromolecule that can be detected via flow cytometry. Additionally, 150kDa FITC-Dextran is similar in size to CRISPR/Cas9 protein which is 160kDa. These experiments suggest that the 3D-printed acoustofluidic system described above may be effective at intracellular delivery of the CRISPR/Cas9 system for gene editing for CAR-T therapy. Further studies are required to assess the ability of functional gene editing with the CRISPR/Cas9 system using the 3D printed acoustofluidic device.

The effects of incubation time, microbubble charge, and immediate washing of cells after acoustofluidic treatment on the intracellular delivery of tracrRNA in HEK293 cells and human lymphocytes Jurkat T-cells are shown above. A fluorescently labeled tracrRNA was used for these studies because tracrRNA is a crucial component of the CRISPR/Cas9 system, which was discussed as a possible solution to reduce the current side effects of CAR-T therapy. Additionally, flow cytometry can be utilized to detect intracellular delivery since the tracrRNA had a fluorophore attached to it. These studies looked at the effects of incubation periods to determine if more extended incubation periods enhanced intracellular delivery. A 48-hour incubation period was chosen because it is the recommended time for current transfection techniques. Two more time points were tested to determine how critical time point is and whether molecular delivery was affected by a prolonged incubation period. There was variance in results between the two cell types at different time points. However, both cell types had significantly higher intracellular delivery of tracrRNA at 48 hours than tracrRNA only, as indicated by ANOVA p-value <0.001 and posthoc analysis. These results suggest that the tracrRNA remained inside the cell 48 hours post-treatment/incubation and washing steps. However, it is possible that the tracrRNA may have degraded after 48 hours as these experiments did not test for intact

tracrRNA. Future studies should test for tracrRNA using PCR testing to determine if the tracrRNA remained intact for 48 hours or if only the fluorophore was inside the cell after 48 hours. In these experiments, acoustofluidic treatment significantly enhanced molecular delivery while maintaining cell viability above 80%. These experiments suggest that RNP, an essential part of the CRISPR/Cas9 system, can be intracellularly delivered to both HEK293 cells and Jurkat T-cells using the 3D printed acoustofluidic system. Similar results were shown in the studies with GFP protein (28kDa) molecular delivery. GFP was chosen as a test molecule because it is a protein that is different in characteristics compared to the other molecules tested. GFP is also a fluorescent molecule that allows for easy analysis through flow cytometry. Successful delivery of a protein with the acoustofluidic system described above is a promising result and affirms the potential use of this non-viral technique for gene editing.

Experimental results of cationic versus neutral microbubble for intracellular delivery of tracrRNA in both HEK293 and Jurkat T-cells were similar. In both cell lines, cationic microbubbles significantly increased intracellular delivery of tracrRNA. However, in HEK293 cells, the cationic microbubbles enhanced intracellular delivery with or without acoustofluidic treatment, and in Jurkat T-cells, only the acoustofluidic treated group had significantly higher intracellular delivery. These results demonstrate that cationic microbubbles alone without ultrasound treatment may be sufficient to induce intracellular delivery of tracrRNA in HEK293 cells. This can be explained due to the cationic/anionic interaction between the microbubbles and cell surface/tracrRNA. Some intracellular uptake of tracrRNA may be induced because of this interaction and prolonged incubation time which is sufficient for endocytosis. However, washing the cells immediately after

acoustofluidic treatment significantly reduced intracellular delivery of tracrRNA in both HEK293 cells and Jurkat T-cells. Washing cells immediately after acoustofluidic treatment and before incubation reduced fluorescent intensity across all groups for both cell lines. A possible explanation for this could be the immediate removal of cationic microbubbles that may be attached to the cell surface, which may promote uptake over time with cellular mechanisms. These results indicate that it may cationic microbubbles, and flow treatment without ultrasound may induce molecular uptake alone.

IV. CONCLUSIONS

This thesis provides new findings regarding acoustofluidic meditated molecular delivery in multiple cell lines. A 3D-printed acoustofluidic device was utilized for intracellular molecular delivery of macromolecule 150kDa FITC-Dextran in four different cell types: Jurkat T-cells, MDA-MB-231 cells, A549 cells, and HEK 293 cells. Results of these studies indicated that there is an optimal range of cationic microbubble concentration for enhanced intracellular delivery without compromising viability of most cells. Microbubble concentration of 5% v/v proved to be most efficient for all cell types compared to lower and higher concentrations. Additionally, these studies demonstrated that acoustofluidic mediated molecular delivery of macromolecules is possible with the 3D printed system in multiple cell lines. Since 150kDa FITC-Dextran and CRISPR/Cas9 protein is similar in size, the 3D printed acoustofluidic system holds promise for a novel non-viral transfection method for CAR-T cell processing.

Additional studies were conducted to test the efficiency of the 3D printed acoustofluidic device for intracellular molecular delivery of a fluorescently labeled tracrRNA in HEK293 cells and Jurkat T-cells. Several parameters were assessed in these studies: the effects of time points on molecular delivery, the effects of cationic microbubbles compared to neutral microbubbles on molecular delivery, and the effects of washing cells post acoustofluidic treatment on molecular delivery. Intracellular delivery of tracrRNA was significantly enhanced with cationic microbubbles with or without acoustofluidic treatment in both cell lines at all three-time points (0hr, 24hr, 48hr). These results indicate that our 3D printed acoustofluidic device with cationic microbubbles can provide rapid intracellular take up of molecules such as tracrRNA. Cationic microbubbles

with acoustofluidic treatment proved to be more effective at intracellular molecular delivery of tracrRNA in both cell lines in comparison to neutral microbubbles with acoustofluidic treatment. Studies also revealed that washing cells post acoustofluidic treatment prevented intracellular uptake of tracrRNA in both cell lines. These results indicate that cationic microbubbles are essential for optimal intracellular uptake of genetic materials such as tracrRNA, essential for gene editing. Thus, combining cationic microbubbles with the 3D printed acoustofluidic system described in this thesis holds the potential to be used as a non-viral transfection method for the CRISPR/Cas9 system since effective delivery of both tracrRNA and a macromolecule that is comparable to cas9 were demonstrated in this study.

Future Recommendations

Future studies should focus on assessing the functional delivery of biological molecules such as proteins, DNA, and RNA into Jurkat T-cells using the 3D-printed acoustofluidic device. Insights garnered in this study, such as optimal microbubble concentrations and effects of washing cells post-treatment, should be utilized to format future studies. Additionally, studies should consider the effect of cationic microbubbles on inducing molecular uptake with more experiments. Microbubble characteristics such as size, shape, and formulations should be explored more to understand some of the results of this thesis more thoroughly. Furthermore, studies should be conducted to determine the ideal tracrRNA to microbubble lipid concertation. There will likely be a threshold of tracrRNA concentration before microbubble size and shape are deformed. In addition, the surface area (~ 3-28 μm^2 for microbubble diameter of ~ 1-3 μm) of the microbubbles limits how much tracrRNA can be attached to the microbubble before it is completely saturated.

Thus, finding the optimal tracrRNA to microbubble ratio is important to optimize molecular delivery.

Additional studies should focus on showing the functional delivery of proteins, DNA, and RNA. A gene cleavage assay can serve as an indicator of functional gene editing. Two components are needed to perform functional genome editing with CRISPR-Cas9: a guide RNA (gRNA) and Cas9 (cleavage protein). Guide RNA(gRNA) consists of CRISPR RNA(crRNA), which indicates the specific DNA target sequence, and a transactivating crRNA(tracrRNA) which binds to the crRNA and Cas9 protein to form a ribonucleoprotein complex. gRNA along with Cas9 protein should be intracellularly delivered to Jurkat T-cells using the 3D printed acoustofluidic system with cationic microbubbles. After 48 hours of incubation, cells should be harvested and prepared for DNA isolation. Standard protocol or DNA isolation kits should be utilized to break open the cells and extract only the DNA. Then, the DNA needs to be expanded using polymerase chain reaction (PCR), which allows for the copying of specific regions of the DNA with sequence-specific primers. The crRNA-specific target sequence should be chosen for PCR. Finally, gel electrophoresis is to be performed to isolate the nucleic acids based on size and charge. The gel is stained with a dye that allows for nucleic acid fragments to be visible as bands. If the target-specific fragment bands are visible, then genome editing was successful. Since the current studies only prove intracellular delivery of biological molecules and not functional gene editing. As mentioned above, with the current studies, it is not possible to determine whether the tracrRNA had degraded at 48 hours and only the fluorophore was inside the cell. Flow cytometry was utilized to detect intracellular fluorescence; however, moving forward, advanced techniques such as confocal microscopy should be used to determine the location

of the tracrRNA. Another limitation of the current study is the lack of studies on the effects of temperature, cell cycle phase, and cell culture techniques on acoustofluidic mediated molecular delivery. Higher temperatures could increase both diffusion and metabolic rate, which may increase endocytic uptake [25, 27]. Thus, studies should be performed at various temperatures to assess how it influences acoustofluidic mediated molecular delivery. Another limitation of the current studies is the lack of focus on ultrasound parameters. Ultrasound parameters such as frequency, pressure, and time under ultrasound treatment may impact intracellular delivery. In addition, studies should be conducted to assess how cationic microbubbles alone without ultrasound may be inducing intracellular delivery. Further studies are required to understand this phenomenon and its ramifications on the 3D-printed acoustofluidic system. If cationic microbubbles prove to be effective at efficiently delivering molecules to cells, then design changes may be required to the current system. Lastly, these studies should be used to create a protocol for acoustofluidic mediated molecular delivery in primary T-cells. Studies with primary T-cells should be conducted once an optimized protocol is developed for acoustofluidic mediated molecular delivery of gene editing compounds. Suppose these studies show successful genome editing with the 3D printed acoustofluidic system with cationic microbubbles. In that case, this system may address the current limitations of viral and non-viral transfection techniques, which limits the use of CAR-T and other immunotherapies. Additional testing and development may allow for the 3D-printed acoustofluidic system to be used for gene editing for immunotherapies such as CAR-T to treat cancer and other diseases.

REFERENCES

1. Miliotou, A.N. and L.C. Papadopoulou, *CAR T-cell Therapy: A New Era in Cancer Immunotherapy.* Curr Pharm Biotechnol, 2018. **19**(1): p. 5-18.
2. Kallam, A. and J.M. Vose, *Recent Advances in CAR-T Cell Therapy for Non-Hodgkin Lymphoma.* Clin Lymphoma Myeloma Leuk, 2019. **19**(12): p. 751-757.
3. Susanibar-Adaniya, S. and S.K. Barta, *2021 Update on Diffuse large B cell lymphoma: A review of current data and potential applications on risk stratification and management.* Am J Hematol, 2021. **96**(5): p. 617-629.
4. Han, D., et al., *Current Progress in CAR-T Cell Therapy for Hematological Malignancies.* J Cancer, 2021. **12**(2): p. 326-334.
5. Mikkilineni, L. and J.N. Kochenderfer, *CAR T cell therapies for patients with multiple myeloma.* Nat Rev Clin Oncol, 2021. **18**(2): p. 71-84.
6. Marofi, F., et al., *A Deep Insight Into CAR-T Cell Therapy in Non-Hodgkin Lymphoma: Application, Opportunities, and Future Directions.* Frontiers in immunology, 2021. **12**: p. 681984-681984.
7. Annesley, C.E., et al., *The Evolution and Future of CAR T Cells for B-Cell Acute Lymphoblastic Leukemia.* Clin Pharmacol Ther, 2018. **103**(4): p. 591-598.
8. Piscopo, N.J., et al., *Bioengineering Solutions for Manufacturing Challenges in CAR T Cells.* Biotechnology journal, 2018. **13**(2): p. 10.1002/biot.201700095.
9. Ramamoorth, M. and A. Narvekar, *Non viral vectors in gene therapy- an overview.* Journal of clinical and diagnostic research : JCDR, 2015. **9**(1): p. GE01-GE6.

10. Fus-Kujawa, A., et al., *An Overview of Methods and Tools for Transfection of Eukaryotic Cells in vitro.* Frontiers in Bioengineering and Biotechnology, 2021. **9**.

11. Nayerossadat, N., T. Maedeh, and P.A. Ali, *Viral and nonviral delivery systems for gene delivery.* Adv Biomed Res, 2012. **1**: p. 27.

12. Yang, Y., et al., *Mechanisms underlying sonoporation: Interaction between microbubbles and cells.* Ultrasonics Sonochemistry, 2020. **67**.

13. DiTommaso, T., et al., *Cell engineering with microfluidic squeezing preserves functionality of primary immune cells in vivo.* Proceedings of the National Academy of Sciences, 2018. **115**(46): p. E10907-E10914.

14. Dressaire, E. and A. Sauret, *Clogging of microfluidic systems.* Soft Matter, 2017. **13**(1): p. 37-48.

15. Razeghian, E., et al., *A deep insight into CRISPR/Cas9 application in CAR-T cell-based tumor immunotherapies.* Stem Cell Research & Therapy, 2021. **12**(1): p. 428.

16. Gao, Q., et al., *Therapeutic potential of CRISPR/Cas9 gene editing in engineered T-cell therapy.* Cancer medicine, 2019. **8**(9): p. 4254-4264.

17. Salas-Mckee, J., et al., *CRISPR/Cas9-based genome editing in the era of CAR T cell immunotherapy.* Hum Vaccin Immunother, 2019. **15**(5): p. 1126-1132.

18. Murphy, E.M., *NON-VIRAL TRANSFECTION EFFICIENCIES FOR THE ADVANCEMENT OF CAR-T THERAPY.* 2019, University of Louisville.

19. Kopechek, J.A., et al., *Ultrasound and Microbubble-targeted Delivery of a microRNA Inhibitor to the Heart Suppresses Cardiac Hypertrophy and Preserves Cardiac Function.* Theranostics, 2019. **9**(23): p. 7088-7098.

20. Centner, C.S., et al., *Acoustofluidic-mediated molecular delivery to human T cells with a three-dimensional-printed flow chamber.* J Acoust Soc Am, 2021. **150**(6): p. 4534.

21. Kopechek, J.A., et al., *Cardiac Gene Expression Knockdown Using Small Inhibitory RNA-Loaded Microbubbles and Ultrasound.* PLoS One, 2016. **11**(7): p. e0159751.

22. Kopechek, J.A., et al., *Ultrasound Targeted Microbubble Destruction-Mediated Delivery of a Transcription Factor Decoy Inhibits STAT3 Signaling and Tumor Growth.* Theranostics, 2015. **5**(12): p. 1378-87.

23. Myrset, A.H., et al., *Design and characterization of targeted ultrasound microbubbles for diagnostic use.* Ultrasound Med Biol, 2011. **37**(1): p. 136-50.

24. Ooi, A., et al., *A Guide to Transient Expression of Membrane Proteins in HEK-293 Cells for Functional Characterization.* Front Physiol, 2016. **7**: p. 300.

25. Bag, N., D.H.X. Yap, and T. Wohland, *Temperature dependence of diffusion in model and live cell membranes characterized by imaging fluorescence correlation spectroscopy.* Biochimica et Biophysica Acta (BBA) - Biomembranes, 2014. **1838**(3): p. 802-813.

26. Centner, C.S., et al., *Ultrasound-induced molecular delivery to erythrocytes using a microfluidic system.* Biomicrofluidics, 2020. **14**(2).

27. Ducommun, P., et al., *Monitoring of temperature effects on animal cell metabolism in a packed bed process.* Biotechnology and Bioengineering, 2002. **77**(7): p. 838-842.

CURRICULUM VITA

Riyakumari Patel received her B.S. in Bioengineering from the University of Louisville in May 2021. During the fall of 2018, she began her first co-op placement under Dr. Jonathan Kopechek. Throughout her three co-op rotations, Riya's primary focus was on the acoustofluidic mediated delivery of small molecules and proteins for improved non-viral transfection techniques for improved cell therapy processing. She was also involved with a project collaborating with Dr. Michael Menze in the Biology Department at the University of Louisville. In this project, she worked on an acoustofluidic flow system for the long-term preservation of red blood cells. Following her graduation in May 2021, Riya began completing her Master of Engineering degree in Bioengineering at the University of Louisville under Dr. Jonathan Kopechek. Following graduation in May 2022, she will join Bristol Myers Squibb as an associate of the aCTivate program to continue her work in improving cell therapy.